NANO LETTERS

Letter

pubs.acs.org/NanoLett

Spectral Modifications and Polarization Dependent Coupling in Tailored Assemblies of Quantum Dots and Plasmonic Nanowires

Christian Gruber,* Andreas Trügler, Andreas Hohenau, Ulrich Hohenester, and Joachim R. Krenn

Institute of Physics, Karl-Franzens-University, Universitätsplatz 5, 8010 Graz, Austria

ABSTRACT: The coupling of optical emitters with a nanostructured environment is at the heart of nano- and quantum optics. We control this coupling by the lithographic positioning of a few (1−3) quantum dots (QDs) along plasmonic silver nanowires with nanoscale resolution. The fluorescence emission from the QD-nanowire systems is probed spectroscopically, by microscopic imaging and decay time measurements. We find that the plasmonic modes can strongly modulate the fluorescence emission. For a given QD position, the local plasmon field dictates the coupling efficiency, and thus the relative weight of free space radiation and emission into plasmon modes. Simulations performed with a generic few-level model give very good agreement with experiment. Our data imply that the 2D degenerate emission dipole orientation of the QD can be forced to predominantly emit to one polarization component dictated by the nanowire modes.

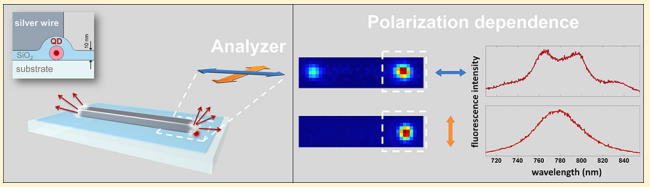

KEYWORDS: *Plasmonics, nanowire, quantum dots, electron beam lithography, coupling, local density of states*

The ability to control single photon emission depends critically on the understanding of the coupling of the emitters to their environment. Matter structured on the wavelength and subwavelength scale can strongly modify excitation and emission rates, radiation patterns, and quantum yield. In particular, nanostructures sustaining surface plasmon modes couple efficiently to emitters due to strong local light enhancement and confinement. Plasmonic nanowires combine nanoscale field confinement with microscale propagation lengths and are thus particularly attractive in this context and hold promise for applications as, for example, photon harvesting and distribution.[1] Single plasmon excitation on nanowires was demonstrated with semiconducting quantum dots (QDs)[2] and nitrogen vacancies in nanodiamonds.[3] The relative positions of wire and emitter were manipulated by a scanning probe to introduce deterministically controlled geometries.[4] Besides plasmon excitation by QDs, the inverse process of addressing QDs by wire plasmons was shown[5,6] and the distance dependence of the coupling of QDs and nanowires was investigated.[7]

In this Letter, we deterministically assemble QDs with silver nanowires by two-step lithography and explore the wavelength, polarization, and position dependence of the fluorescence light. We show how the QD emission is redistributed between nanowire plasmons and free space radiation, and infer a QD emission dominated by the coupling to the nanowire plasmon modes.

The hybrid structures built from QDs and silver nanowires are fabricated by means of two-step electron beam lithography (similar to the methods reported in refs 6 and 8) on glass cover slides decorated with silver marker structures to facilitate the two-step process. For the sake of a more precise alignment, we start with the QD deposition. First, in a 60 nm thick poly(methyl metacrylate) (PMMA) mask, holes with a diameter of 30 nm are lithographically fabricated by local electron exposure and wet-chemical development. A 1 μM QD solution in water (CdSeTe/ZnS, Qdot 800 ITK from Invitrogen) is spin-coated on this mask and after water evaporation we find QDs located in the holes without further processing. The emission maxima of individual QDs range between 775 and 790 nm and the spectral width of the emission band of about 100 nm is broad enough to cover a few plasmon modes of the silver nanowires, which are fabricated in the second lithographic step. After lifting off the PMMA mask, a 10 nm thick SiO_2 film is deposited as a spacer layer to prevent direct quenching of the QD emission due to coupling to nonradiative nanowire plasmon modes. Subsequently, by spin-coating and electron lithography, a further 100 nm thick PMMA mask with the nanowire pattern is added, which is aligned relative to the QD areas guided by marker structures to a precision of about ±10 nm. After development, metal deposition, and a liftoff process, the such fabricated silver wires are 100 nm wide and 4 μm long and the height is set by the deposition of silver of 50 nm mass thickness (monitored by a quartz crystal microbalance). The dimensions are chosen such that all transversal plasmon modes are off-resonant with respect to the QD emission. Finally, another 10 nm thick SiO_2 layer is applied to encapsulate the entire structures from environmental conditions. By the combination of correlation measurements and fluorescence time traces we can determine the number of QDs per hole, a number that we consistently find to be 1−3. As an example, the correlation function measured in a Hanbury Brown and Twiss setup[9] (see below) of a QD area coupled to a

Received: June 1, 2013
Revised: August 5, 2013
Published: August 22, 2013

   dx.doi.org/10.1021/nl4019947 | *Nano Lett.* 2013, 13, 4257−4262

4 μm long nanowire in Figure 1a demonstrates a pronounced dip at zero time delay, which is characteristic for photon

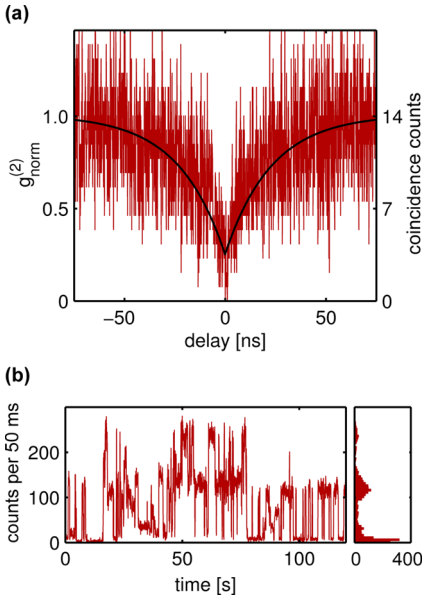

Figure 1. Counting emitters in a QD-nanowire system. (a) Correlation function measured of a QD area coupled to one end of a 4 μm long silver nanowire. The respective fluorescence image is shown in the top image of Figure 5a. (b) Fluorescence intensity time trace of the same QD area including the corresponding histograms on the right.

antibunching. As this dip clearly falls below 0.5, it is tempting to conclude that only a single QD is present. However, the fluorescence intermittency (blinking) characteristic for QDs can give rise to this result as well in the presence of a few QDs. With the approach discussed in ref 6, we conclude that indeed two QDs are present in this specific sample. This is corroborated by the fluorescence time trace of the considered sample plotted in Figure 1b. As evident from the histogram we find two equidistant fluorescence "on" levels, corresponding to one (lower level) and both (upper level) QDs being in the "on" state, supporting the interpretation of two QDs being present.

For fluorescence microscopy and spectroscopy of the QD-nanowire system, the QDs are optically excited by a circularly polarized (to secure isotropic excitation of the QDs) argon ion laser beam (wavelength 488 nm), focused onto the QDs through a microscope objective (100×, 0.95 numerical aperture) to a spot of approximately 400 nm full-width at half-maximum. The fluorescence is detected in epifluorescence geometry and is either imaged by a camera or spectroscopically analyzed by taking spectra from the area of interest. Dichroic components (beam splitter 520 nm long pass, long pass filter 510 nm, band-pass filter 794 ± 80 nm) are used to suppress the excitation light from the images. Optionally, we apply an analyzer in front of the camera. Complementary time-resolved measurements were done using a diode laser (wavelength 487 nm) in time-correlated single photon counting mode and in a Hanbury Brown and Twiss setup.

For characterizing the plasmon modes of the nanowires, we apply dark-field scattering spectroscopy as introduced in ref 10. The light scattered from one nanowire end (right-hand side in the image orientation used throughout) upon plasmon excitation at the other (left-hand) wire end is analyzed. This selective plasmon excitation is achieved in the evanescent field of a prism-coupled, unfocused white light beam totally reflected from the sample surface. The scattered light spectra show distinct peaks that correspond to the Fabry–Perot modes in the nanowire cavity. We note that this method is used for plasmon mode characterization only, not for fluorescence spectroscopy as described above.

The lithographic fabrication scheme allows us to build the QD-nanowire assemblies with high spatial precision and thus to deterministically probe coupling with high lateral resolution. On every single 4 μm long silver nanowire, the QDs are attached to only one predefined area of about 30 nm in diameter laterally centered with respect to the nanowire width. To avoid any coupling to adjacent structures, the distance between different nanowires on one sample is set to 3 μm. We start with the results for QDs at the middle position of a nanowire. The plasmon mode spectrum of the wire is plotted as the black curve in Figure 2a, revealing the plasmonic Fabry–

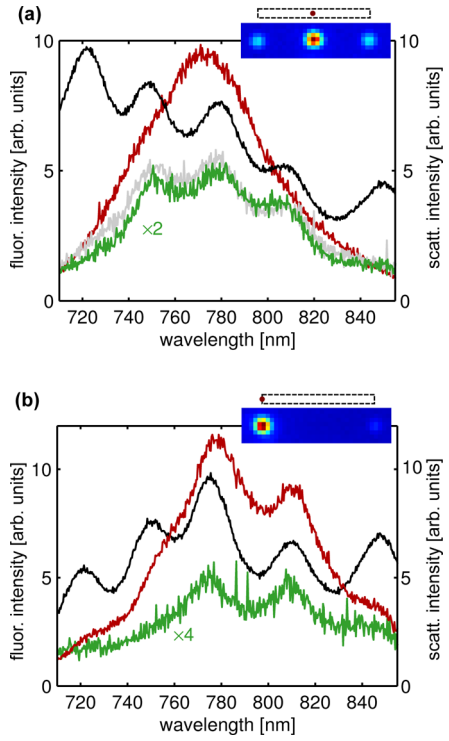

Figure 2. Spectral signatures of QDs coupled to a 4 μm long nanowire for unpolarized detection. The black curves show the nanowire mode spectra acquired by dark-field scattering spectroscopy (ref 10). (a) For QDs located at the wire center, the red spectrum is acquired from the QD area, the gray and green spectra are measured from the left and right nanowire end, respectively. (b) For QDs located at the left nanowire end, the red spectrum is acquired from the QD area, the green spectrum from the right nanowire end. The insets depict schematic drawings and fluorescence images. The minimum and maximum image intensity levels are normalized to the full color range (for color bar see Figure 5) and the quantitative values can be read from the *y*-axis scales of the main graphs.

Perot modes of the wire.[10] The fluorescence of the QDs at the middle position upon direct excitation with the laser is shown by the red curve (Figure 2a, unpolarized detection). Besides this direct QD emission (red curve) we observe spectrally modulated light emission from the nanowire ends (see inset) with identical spectral modulations (gray and green curve).

dx.doi.org/10.1021/nl4019947 | *Nano Lett.* 2013, 13, 4257–4262

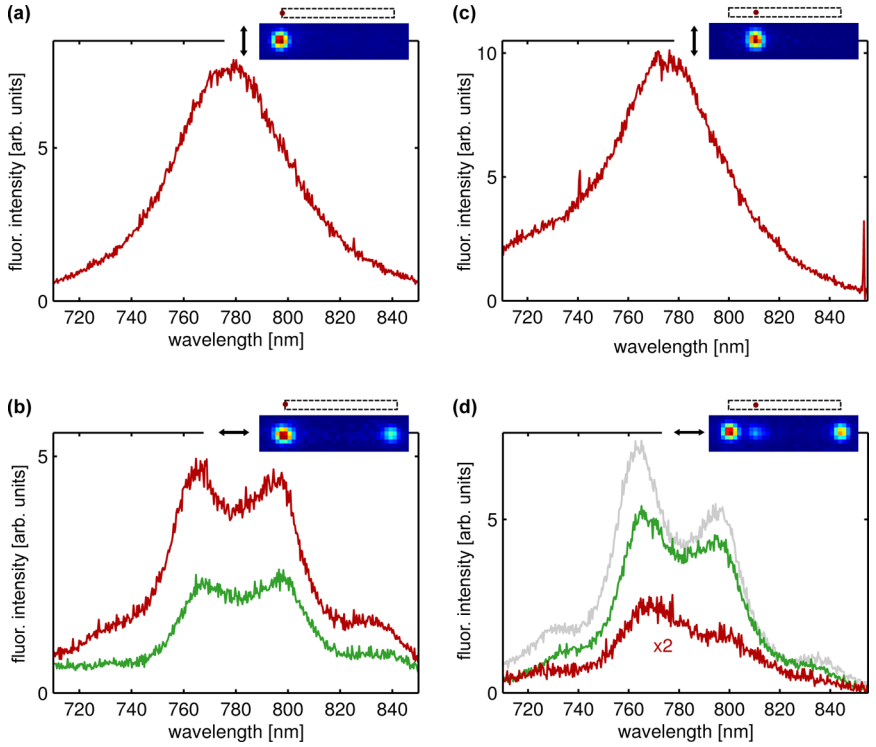

Figure 3. Polarization dependence of fluorescence spectra of QDs coupled to a 4 μm long nanowire. For QDs located at the left nanowire end (a) depicts the spectrum from the QD area for an analyzer orientation in the detection path perpendicular to the nanowire axis. No emission from the right wire end is detectable in this case. (b) For an analyzer orientation parallel to the nanowire axis, the red and green spectra are measured from the left and right nanowire end, respectively. (c,d) The corresponding spectra for QDs located 1 μm from the left end; the red spectra are acquired from the QD area, gray and green spectra from the left and right nanowire ends, respectively. The insets depict schematic drawings and fluorescence images, the double arrows indicate the analyzer orientations. The minimum and maximum image intensity levels are normalized to the full color range (for color bar see Figure 5), the quantitative values can be read from the *y*-axis scales of the main graphs.

These modulations follow precisely the plasmon mode spectrum, which suggests the following interpretation. The QDs excite, through near field coupling, plasmons that propagate toward both wire ends where they are (partly) scattered to light.[6,7,11] We find that only a marginal modulation is discernible in the spectra of the direct emission from the QDs and that their coupling efficiencies to plasmons of even and odd mode number seem roughly identical.

When positioning the QDs at the left nanowire end (Figure 2b) a similar behavior is observed. Again, the emission from both ends is defined by the QD spectrum, which is modulated by the spectral plasmon mode density. The weaker intensity scattered from the right wire end is due to plasmon propagation loss. For this geometry, however, the direct QD emission cannot be separated from scattering at the left nanowire end. This resembles the case of emitters coupled to nanoparticles that act as optical antennas and dominate the emission properties of the subwavelength-sized ensemble.[8] It is noteworthy that we observe identical spectral positions of the emission peaks from both nanowire ends for the present case of near field plasmon excitation by QDs, which can be different in case of far-field excitation.[12]

To investigate the fluorescence emission of the coupled QD-nanowire system in more detail, we add an analyzer to the optical detection path, which enables us to discriminate between contributions from longitudinal and transversal plasmon modes. For the analyzer orientation perpendicular to the wire axis, all detectable fluorescence originates directly from the QD area at the left nanowire end, Figure 3a, and its spectrum shows no modulation. Conversely, fluorescence is observed from both wire ends and the spectra are modulated for the analyzer orientation along the nanowire axis, Figure 3b. If the QDs are positioned along the nanowire (1 μm away from the left wire end), we again observe all fluorescence directly from the QD area for perpendicular analyzer orientation, Figure 3c. For parallel orientation, modulated spectra are measured from both wire ends, as plotted by the gray and green curves in Figure 3d. Some weak fluorescence is detected directly from the QD area (red curve), in this case as well with spectral modulations that coincide with those observed from the wire ends. We interpret this as a result of plasmon modes scattered at the "defect" introduced by the presence of the QD.

To discuss the differences observed for the two analyzer orientations, we first analyze the emission spectra. They can be understood qualitatively by considering the partial local density of optical states (LDOS)[13] offered by the presence of the plasmonic nanowire that depends on the dipole orientation and determines the QD-nanowire coupling. The nanowires have some longitudinal but no transversal plasmon resonances within the wavelength range of the QD emission spectrum.[14] As the QDs are deposited at the lateral center with respect to the nanowire width, components of the QD emission dipole that are parallel to the nanowire or perpendicular to the sample plane can strongly couple to the resonant longitudinal plasmon modes. The direct emission from these polarizations is thus low and the emission from the wire ends peaks at the plasmon mode resonances. For parallel orientation of the analyzer, only

dx.doi.org/10.1021/nl4019947 | *Nano Lett.* 2013, 13, 4257−4262

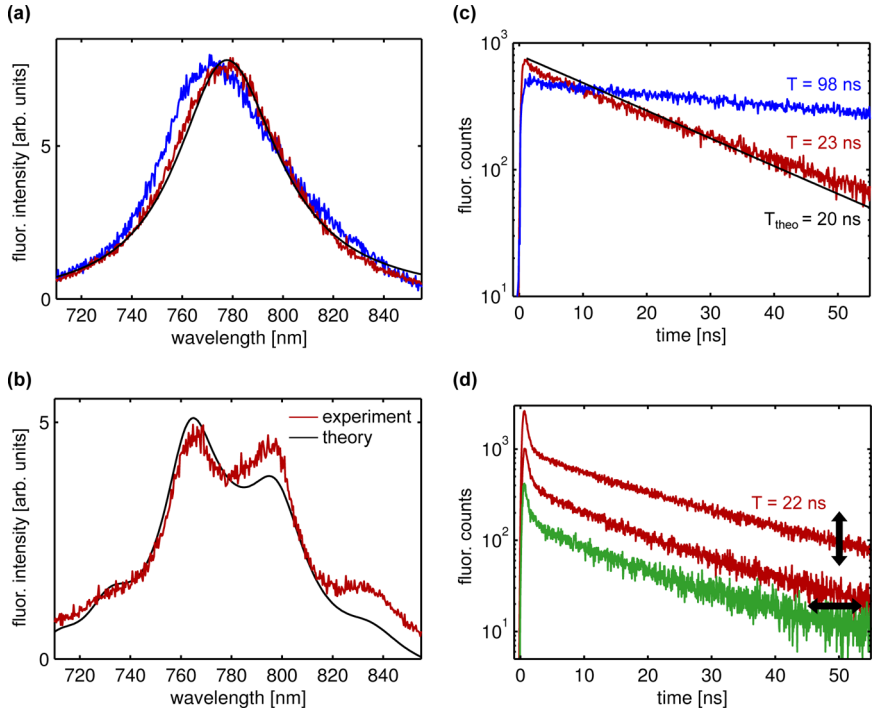

Figure 4. Wavelength, time, and polarization dependence of the QD-nanowire system in Figure 3a,b (red curves) compared to a few-level model of a dipole emitter coupled to an oscillator with discrete energies corresponding to the Fabry−Perot resonances of the 4 μm long silver nanowire. The model (black lines) is fit to the spectra with a QD dephasing time of 6.5 fs. Here, the spectral shape is governed by dephasing, lifetime effects do not noticeably contribute to the line width. (a) Model and experiment for the uncoupled case (analyzer orientation perpendicular to the nanowire axis, Figure 3a), the blue curve shows the normalized QD spectrum on the bare glass substrate. (b) Model and experiment for the coupled system (analyzer orientation parallel to the nanowire axis, Figure 3b). (c) Unpolarized measurement of the fluorescence time decay of QDs on the bare glass substrate (blue) and for the coupled case (red) that corresponds to the structure analyzed in Figure 1. (d) Measurement of the fluorescence time decay with different analyzer orientations. The red curves are measured from the QD area at the left nanowire end, the green curve is measured from the right wire end. The double arrows indicate the analyzer orientations (horizontal for the two lower curves). The marked features at times <2 ns might be indicative of biexciton emission, prominently appearing here due to higher excitation intensities as compared to (c), used to balance signal loss due to the additional analyzer in the detection scheme.

these longitudinal plasmon modes can contribute to the detector signal.

In contrast, the emission dipole components in the sample plane but perpendicular to the nanowire cannot couple to the longitudinal plasmon modes as their electromagnetic fields have a different symmetry with respect to the nanowire axis than the longitudinal modes. Moreover, the coupling to transversal plasmon modes is weak as their resonances are in the blue spectral range.[14] Their response to electromagnetic fields does not peak and their contribution to the LDOS is low within the QD emission spectral range. Thus the emission spectrum for this dipole orientation should be dominated by direct QD emission.

To closer model the coupling and emission process, we employ a simple and generic few-level scheme that is expected to embody the characteristic features of the coupled QD-nanowire system. In our model, we introduce the ground and excited QD states g and e (energies E_g and E_e) and describe the nanowire through a set of plasmonic modes whose energies $\hbar\omega_l$ are extracted from the experimental spectra. The coupled QD-nanowire system is then described by the Hamiltonian

$$H = \sum_{i=g,e} E_i|i\rangle\langle i| + \sum_l \hbar\omega_l a_l^\dagger a_l + g\sum_l (a_l^\dagger|g\rangle\langle e| + a_l|e\rangle\langle g|) \quad (1)$$

where g is the coupling constant between the excited QD state and the plasmonic Fabry−Perot modes. The bosonic field operators $a_l^\dagger$ create a plasmon in mode l. The last term on the right-hand side describes processes where the excitation is promoted from the QD to the plasmon, or vice versa. In addition to the coherent couplings, we introduce a number of scattering-type processes, which we describe within a master equation of Lindblad form[15]

$$\dot{\rho} = -\frac{i}{\hbar}(H_{\text{eff}}\rho - \rho H_{\text{eff}}^\dagger) + \sum_k L_k \rho L_k^\dagger \quad (2)$$

Here $H_{\text{eff}} = H - i/2\sum_k L_k^\dagger L_k$ is an effective Hamiltonian,[15] and L_k are the Lindblad operators for the various scattering processes, including radiative decay and dephasing of the excited QD state, optical QD pumping through off-resonant states, as well as radiative decay and Ohmic losses of the plasmonic modes. Our master equation approach of eq 2 allows us to compute both the fluorescence spectra under cw-excitation, by employing the quantum regression theorem,[15] as well as the fluorescence decay after a short excitation pulse. Throughout we assume weak optical pumping, such that either only the QD or plasmon mode is excited at one instant of time. Under such conditions, we expect no significant modifications of our results for systems consisting of a few QDs.

We now apply our model to the experimental data of Figure 3a,b with a decay time of 98 ns as an input parameter that is experimentally determined from QDs on the bare glass substrate (Figure 4c, blue curve). Assuming a QD dephasing

dx.doi.org/10.1021/nl4019947 | Nano Lett. 2013, 13, 4257−4262

time of 6.5 fs and neglecting plasmonic coupling we find an almost perfect agreement between the simulated spectrum (black) and the experimental result (red) for the case of perpendicular analyzer orientation, Figure 4a. This demonstrates that our QD emission is governed by homogeneous broadening at the room-temperature conditions of our experiments. This is in marked contrast to observations on QD ensembles, where the spectra are dominated by inhomogeneous broadening.[16] Because of solely homogeneous broadening, the spectrally selective coupling of the emission dipole to the longitudinal plasmon modes cannot alter the QD emission spectrum for perpendicular dipole orientation (along the *y*-axis according to the schematic drawing in Figure 5a), as

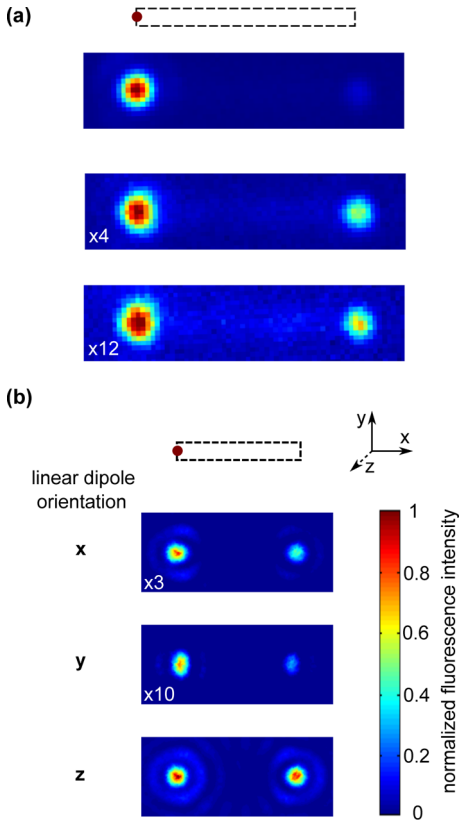

Figure 5. Influence on the dipole plane orientation on the coupling to the nanowire. (a) Fluorescence images (unpolarized) of nominally identical systems built from 4 μm long nanowire and QDs at the left wire end. In the topmost image, only 2 QDs are present as the fluorescence decay time analysis shown in Figure 1 reveals. (b) Simulated fluorescence images of linear dipoles orientated along the three principal axis *x*, *y*, and *z*, respectively, coupled to a 2 μm long nanowire. All fluorescence images are normalized to the maximum intensity. The intensity of some images is scaled (multiplied) by the white number indicated in the image to meet the same color bar.

both decay channels deplete the same excited state. This and the weak coupling to plasmon modes for this dipole orientation is corroborated by the very good correspondence of the observed spectrum (red) with the spectrum of QDs on the bare glass substrate (blue).

For analyzing the spectra observed for parallel analyzer orientation we use detunings of −0.11, −0.04, 0.03, 0.10, and 0.15 eV for the plasmon modes with respect to the QD resonance at a wavelength of 780 nm. We set the QD-nanowire coupling strength to 20 μeV and assume a 12 fs plasmon decay time. It is gratifying to see from Figure 4b that our generic few-level model reproduces all essential features observed in the experimental fluorescence spectrum measured for parallel analyzer orientation. In addition, the same parameter set also yields a good fit for the temporal QD population decay of 20 ns, plotted by the black line in Figure 4c, which provides a direct measure of the LDOS. Comparing the experimental decay times of the QDs on a bare substrate with the QDs coupled the left nanowire end, a LDOS contrast of 4−5 can be deduced. Figure 4d shows the same decay times for both analyzer orientations and for both wire ends. Here a higher excitation intensity is used to compensate signal loss due to the additional analyzer in the detection scheme. The short decay components <2 ns might be indicative of biexciton emission that appears as the excitation intensity is increased.

To understand the observed monoexponential decay with identical decay times for both analyzer orientations, the specific properties of QD fluorescence have to be considered. Generally speaking, the absorption of a CdSeTe/ZnS QD is isotropic, but the QD emission dipole is 2D degenerate within the "bright plane" perpendicular to the "dark axis" of the wurzite lattice.[17,18] In the experiment, the orientation of the dark axis is beyond control and no preferential orientation could be observed by comparing images and emission diagrams of several lithographically positioned QDs. The orientation varies but is randomly distributed. To illustrate the influence of the emitter's dipole orientation on the coupling to the nanowire, we summarize in Figure 5b fluorescence images of hybrid systems simulated with the MNPBEM toolbox[19] for differently orientated linear dipole emitters, with a transition wavelength of 780 nm, laterally positioned at the nanowire end and vertically displaced by 15 nm from the wire, in accordance to the fabricated structures. Because of the finer boundary discretization in the vicinity of the QDs (we use ∼21 000 boundary elements) we were limited to 2 μm long nanowires, which, however, is not expected to impact the qualitative comparison between simulation and experiment. Figure 5b shows simulation results where the dipoles are oriented along the three principal axes *x*, *y*, and *z*. The (unpolarized) images of the dipole-nanowire emission are computed by using the angular spectrum representation of focal fields,[13] a procedure that mimics the working principle of an optical microscope. We observe that the emission patterns as well as the intensities vary between the different dipole orientations, which results from the different dipole-nanowire coupling strengths. The experimental fluorescence images in Figure 5a show three nominally identical QD-nanowire systems with the QDs located at the left end of the nanowire. The respective fluorescence decay time analysis of the topmost image reveals that two QDs are present at this structure. As we find quite different intensities and coupling efficiencies (deduced from the ratio of the fluorescence signals at both wire ends) similar to the simulations, we expect differently oriented QDs in the respective structures to be the main source for the observed differences. The QD positional variations are below 20 nm and have only minor influence on the coupling strength, as the variations of the LDOS on this length scale are low. The much weaker fluorescence intensities of the middle and bottom images in Figure 5a as compared to the top image (including 2 QDs) makes it highly likely that these structures include single QDs. From complementary polarization microscopy measurements of single QDs,[17] we find that the QD orientation and

dx.doi.org/10.1021/nl4019947 | *Nano Lett.* 2013, 13, 4257−4262

thus the associated 2D dipole plane orientation on our samples does not change in time.

After optical excitation to a higher excited state of the QD, internal conversion to the lowest excited state takes place. As the emission dipole is degenerated in the bright plane, one might assume two orthogonally polarized, energetically degenerated excited states. As the partial LDOS depends on the dipole orientation, different coupling of these excited states to the nanowire plasmon modes can be anticipated, provided that their symmetry plane does not coincide with a symmetry plane of the nanowire. For the experimental case, this coincidence is very unlikely, as the QD bright plane orientation with respect to the nanowire is completely random. Consequently, the decay times of the two orthogonally polarized states should differ and one would observe a multiexponential fluorescence decay. However, all our results show an almost monoexponential decay with no dependence on the analyzer orientation (deviations are within the experimental uncertainty), although the fluorescence lifetime is shortened by a factor on the order of 5 and clear signatures of a multiexponential decay would be expected. This allows to conclude that both orthogonally polarized excited states couple identically to the environment.

This is further corroborated by the observed fluorescence intensities. Consider the extreme case where one of the polarization states is coupled exclusively to the longitudinal nanowire modes, whereas the other one is basically uncoupled due to its orientation perpendicular to the wire. After excitation, the two orthogonal polarization states of the QD become equally populated (the presence of the nanowire is not expected to influence the internal conversion process in our weak coupling regime) and decay with different rates. For weak excitation, the fluorescence intensity is solely governed by the quantum yield, which is lower for the coupled polarization state due to Ohmic plasmon losses resulting in a stronger fluorescence from the uncoupled state. If both polarization states couple equally to the nanowire, they both transfer their energy with a larger probability to the plasmonic modes and the corresponding fluorescence intensity becomes enhanced. This is what we observe in our experiments. By considering damping of the nanowire plasmons that are estimated from the experimentally determined propagation losses,[20] we deduce that the decay to plasmon modes (detected for analyzer orientation parallel to the long nanowire axis) is at least a factor of 2 more probable than the direct emission (detected for perpendicular orientation). This value stems from the fluorescence intensities of both QD-nanowire configurations represented in Figure 3. Note that the air objective detects only part of the scattered plasmons that are emitted at large angles[21] while most of the directly emitted light from the QD is collected. Our results imply that the two orthogonally polarized exited states in the QD couple almost identically to the anisotropic environment, and that the large contrast between the partial LDOS for the different dipole orientations defines the emission characteristic of the QDs.[8]

In conclusion, we have optically analyzed the electrodynamic coupling in systems deterministically built from single to a few QDs and plasmonic nanowires. This coupling is spectrally modulated due to the plasmon mode spectrum, as observed by plasmon scattering at the wire ends. The essence of the coupling process can be captured in a simple few-level model, and we could demonstrate that the 2D polarization degeneracy of the QD emission dipole is untouched by the polarization-dependent partial LDOS of the nanowire. If the QD's dark axis orientation supports coupling to a plasmon mode, this channel strongly depletes the QD's excited state on the cost of the excitation of other modes. Both orthogonal emission dipole states of the QD contribute equally to this process.

AUTHOR INFORMATION

Corresponding Author

*E-mail: ch.gruber@uni-graz.at.

Notes

The authors declare no competing financial interest.

ACKNOWLEDGMENTS

Financial support is acknowledged from the European Union under project no. ICT-FET 243421 ARTIST and the Austrian Science Fund FWF under project P24511−N26 and the SFB NextLite.

REFERENCES

(1) Chang, D. E.; Sørensen, A. S.; Hemmer, P. R.; Lukin, M. D. *Phys. Rev. Lett.* **2006**, *97*, 1−4.
(2) Akimov, A. V.; Mukherjee, A.; Yu, C. L.; Chang, D.; Zibrov, A. S.; Hemmer, P.; Park, H.; Lukin, M. D. *Nature* **2007**, *450*, 402−406.
(3) Kolesov, R.; Grotz, B.; Balasubramanian, G.; Hemmer, P. R.; Jelezko, F.; Wachtrup, J. *Nat. Phys.* **2009**, *5*, 470.
(4) Huck, A.; Kumar, S.; Shakoor, A.; Andersen, U. L. *Phys. Rev. Lett.* **2010**, *096801*, 5.
(5) Wei, H.; Ratchford, D.; Li, X. E.; Xu, H.; Shih, C.-K. *Nano Lett.* **2009**, *9*, 4168−4171.
(6) Gruber, C.; Kusar, P.; Hohenau, A.; Krenn, J. R. *Appl. Phys. Lett.* **2012**, *100*, 231102.
(7) Fedutik, Y.; Temnov, V. V.; Schöps, O.; Woggon, U.; Artemyev, M. V. *Phys. Rev. Lett.* **2007**, *99*, 136802.
(8) Curto, A. G.; Volpe, G.; Taminiau, T. H.; Kreuzer, M. P.; Quidant, R.; van Hulst, N. F. *Science* **2010**, *329*, 930.
(9) Hanbury Brown, R.; Twiss, R. Q. *Nature* **1956**, *177*, 27−29.
(10) Ditlbacher, H.; Hohenau, A.; Wagner, D.; Kreibig, U.; Rogers, M.; Hofer, F.; Aussenegg, F. R.; Krenn, J. R. *Phys. Rev. Lett.* **2005**, *95*, 257403.
(11) Wang, L.-L.; Zou, C.-L.; Ren, X.-F.; Liu, A.-P; Lv, L.; Cai, Y.-J.; Sun, F.-W.; Guo, G.-C.; Guo, G.-P. *Appl. Phys. Lett.* **2011**, *99*, 061103.
(12) Hohenau, A.; Kusar, P.; Gruber, C.; Krenn, J. R. *Opt. Lett.* **2012**, *37*, 746−748.
(13) Novotny, L.; Hecht, B. *Principles of Nano-Optics*; Cambridge University Press: Cambridge, 2006.
(14) Schider, G.; Krenn, J. R.; Gotschy, W.; Lamprecht, B.; Ditlbacher, H.; Leitner, A.; Aussenegg, F. R. *J. Appl. Phys.* **2001**, *90*, 3825−3830.
(15) Walls, D. F.; Milburn, G. F. *Quantum Optics*; Springer: Berlin, 2007.
(16) Jacak, L.; Hawrylak, P.; Wojs, A. *Quantum Dots*; Springer: Berlin, 1998.
(17) Empedocles, S. A.; Neuhauser, R.; Bawendi, M. G. *Nature* **1999**, *399*, 126−130.
(18) Koberling, F.; Kolb, U.; Philipp, G.; Potapova, I.; Basche, T.; Mews, A. *J. Phys. Chem. B* **2003**, *107*, 7463−7471.
(19) Hohenester, U.; Trügler, A. *Comput. Phys. Commun.* **2012**, *183*, 370.
(20) Kusar, P.; Gruber, C.; Hohenau, A.; Krenn, J. R. *Nano Lett.* **2012**, *12*, 661−665.
(21) Shegai, T.; Miljkovic, V. D.; Bao, K.; Xu, H.; Nordlander, P.; Johannsen, P.; Käll, M. *Nano Lett.* **2011**, *11*, 706−711.